

Supporting information

Gyroidal MOFs: Anion Coordination Effect Enables Inverse Architecture and Enhanced Moisture Stability

Guo-Jian Ren,^a Na Li,^{*a,b} Nan Lu,^a Qiang Gao,^a Ying-Hui Zhang,^a Xuemin Wang,^a Ze Chang,^a Yan-Qing Liu,^a and Xian-He Bu^{a,b}

*Corresponding author. E-mail: lina@nankai.edu.cn

CONTENTS

S1. The valence state calculation

S2. Adsorption measurements

S3. DFT theoretical calculations

S4. Vacuum treatment of fresh crystal of GMOF-2

S5. Structural figures, supplementary characterizations

S1. The valence state calculation

The valence of a bond between two atoms, *i* and *j* is given by S_{ij} . The sum of S_{ij} is the valence of the *i* atom. The calculated results are shown in the table 1.^[S1]

$$V_i = \sum_j S_{ij} = \sum_j \exp\left(\frac{r_0 - r_{ij}}{B}\right)$$

Table S1. Bond valence sum (BVS) of there GMOFs

	GMOF-1		GMOF-2		GMOF-3	
	V _{Co^{II}}	V _{Co^{III}}	V _{Co^{II}}	V _{Co^{III}}	V _{Co^{II}}	V _{Co^{III}}
Co1	1.730	1.982	1.818	2.081	1.866	2.145
Co2	1.637	2.006	1.628	1.997	1.701	2.084
Co3	1.516	1.708	1.516	1.796	1.798	1.958

S2. Adsorption measurements

The samples were treated with supercritical CO₂ in a Tousimis™ Samdri® PVT-30 critical point dryer. Prior to drying, the DMA solvated samples were soaked in absolute ethanol to exchange the occluded solvent for C₂H₅OH for 48 h. Then the ethanol-containing samples were placed inside the dryer and the ethanol was exchanged with CO₂ (liquid) over a period of 6 hours according to literature.^[S2]

The processed samples were loaded in sample tubes and activated under high vacuum (less than 10⁻⁵ Torr) at 60 °C for GMOF-2 and GMOF-3. Degassed samples were used for gas sorption measurements. Gas adsorption measurements were performed using an ASAP 2020 M gas adsorption analyzer.

The N₂ sorption isotherms were collected at 77 K in a liquid nitrogen bath. The CO₂ sorption isotherms were collected at 273 K in an ice water mixture bath, and a water bath was used for adsorption isotherms at 298 K as the center-controlled air conditioner was set up at 25 °C. The measurements of H₂O were preceded at 273 K in an ice water mixture bath, and a water bath was used for adsorption isotherms at 298 K as the center-controlled air conditioner was set up at 25 °C.

S3. DFT theoretical calculations

The theoretical calculations of the adsorption of H₂O molecule by coordination polymer were carried out by DFT theoretical calculation with wB97XD^[S3] functional

in Gaussian 09^[S4] program package. The 6-31G(d) basis set for all nonmetal atoms and Lanl2DZ basis set and pseudo potential for Co(II) ion were adopted in calculation. Based on crystal data, two structure units, the trinuclear and dinuclear cluster, were constructed for theoretical calculation, where the organic ligand was replaced by pyridine and methyl-tetrazole for saving computation time.

Table S2. Average bond order

Building block		Mayer bond order	Wiberg bond order	Natural bond order
Trinuclear cluster	Br-coordinated	2.185	1.631	2.138
	Non-coordinated	2.055	1.549	2.087
Dinuclear cluster	NO ₃ ⁻ -coordinated	2.082	1.705	2.440
	Non-coordinated	2.066	1.646	2.340

Predicted in Wb97xd/6-31G(d)-Lanl2DZ theoretical level

S4. Vacuum treatment of fresh crystal of GMOF-2

To confirm the sensibility of GMOF-2 toward H₂O molecules, the fresh blue crystals were put into the vacuum drier and some water was placed at the bottom of the drier. When the vacuum degree reached the 0.99, the crystals were gradually turned into red. As the water was poured out, the crystals became blue again before vacuum degree reached the 0.99.

References

- S1. J. H. Jia, X. Lin, C. Wilson, A. J. Blake, N. R. Champness, P. Hubberstey, G. Walker, E. J. Cussen, M. Schröder, Twelve-connected porous metal–organic frameworks with high H₂ adsorption, *Chem. Commun.* 2007, **8**, 840-842.
- S2. A. P. Nelson, O. K. Farha, K. L. Mulfort, J. T. Hupp, Supercritical processing as a route to high internal surface areas and permanent microporosity in metal-organic framework materials, *J. Am. Chem. Soc.* 2009, **131**, 458-460.
- S3. J. D. Chai, M. Head-Gordon, Long-range corrected hybrid density functionals with damped atom–atom dispersion corrections, *Phys. Chem. Chem. Phys.* 2008, **10**, 6615-6620.
- S4. *Gaussian 09, Revision B.01*: Frisch, M. J. *et al.* Gaussian, Inc.: Wallingford, CT, **20**.

S5. Structural figures, supplementary characterizations

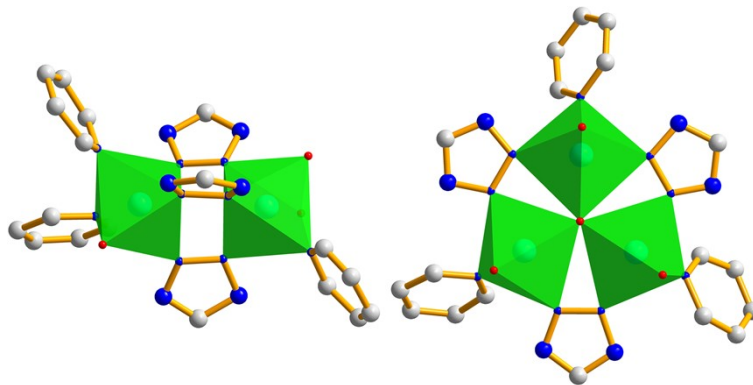


Fig. S1 Coordination configurations of SBU(I) and SBU(II) in GMOF-1 (gray C, blue N, red O, green Co, while H atoms were omitted for simplification).

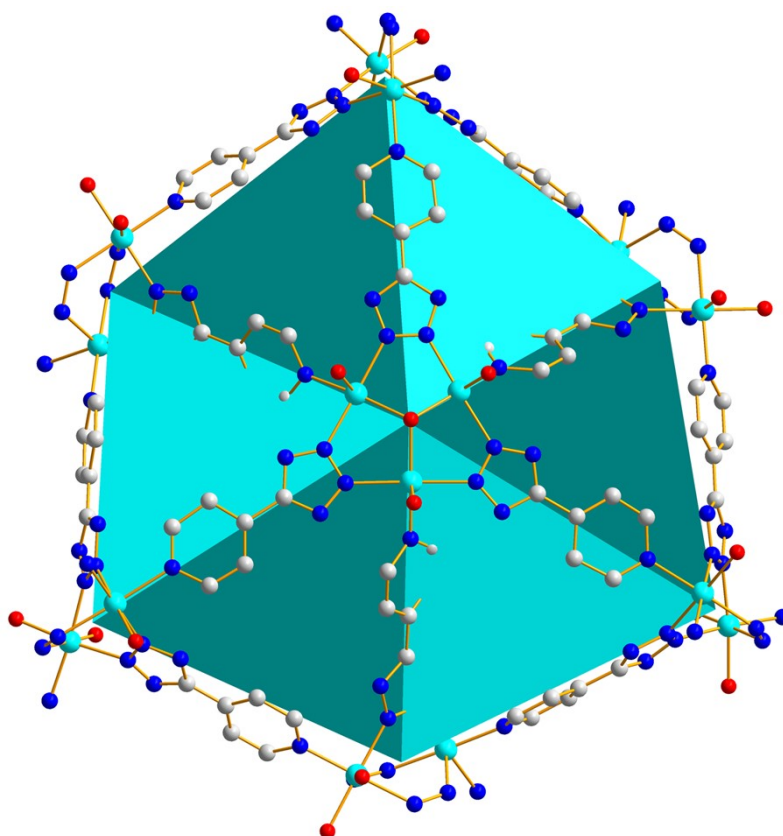


Fig. S2 Non-planar hexagon built by the connection of one SBU (I), six SBU(II), and 4-Ptz ligands in GMOF-1.

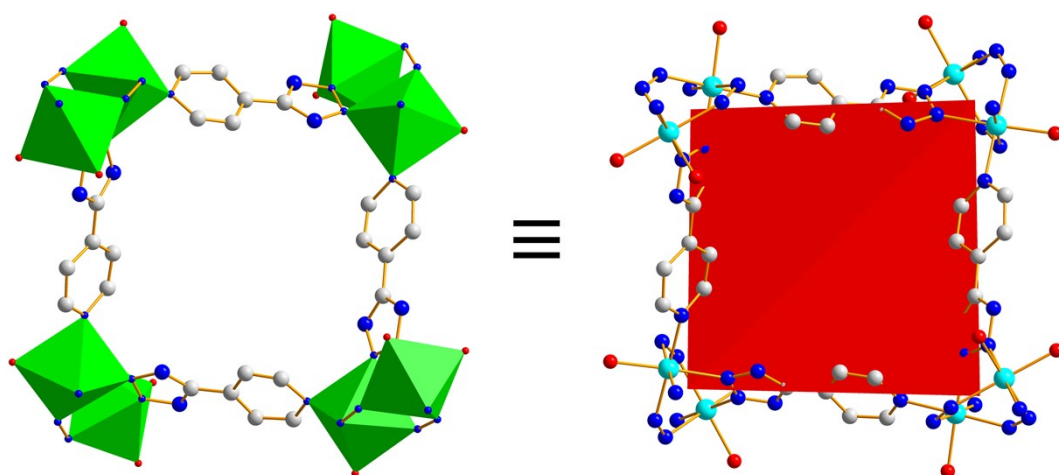


Fig. S3 Twisted quadrangle constructed by the connection of four SBU (II) and 4-Ptz ligands in GMOF-1.

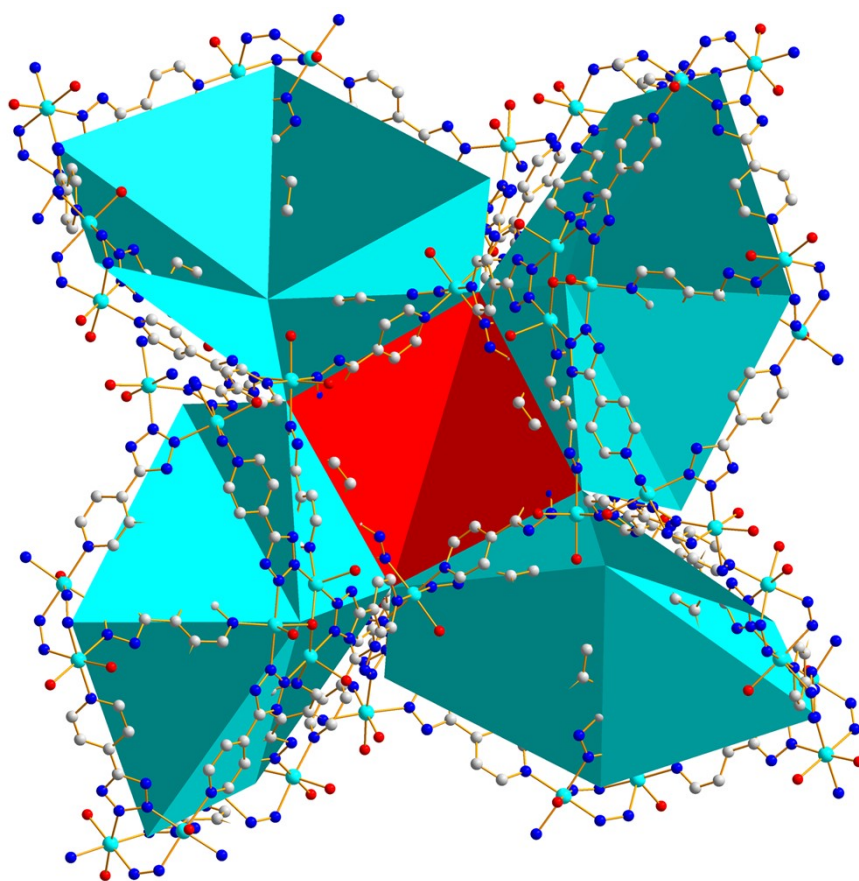


Fig. S4 Four-vaned windmill constructed by double-vertex shared mode of non-planar hexagons in GMOF-1.

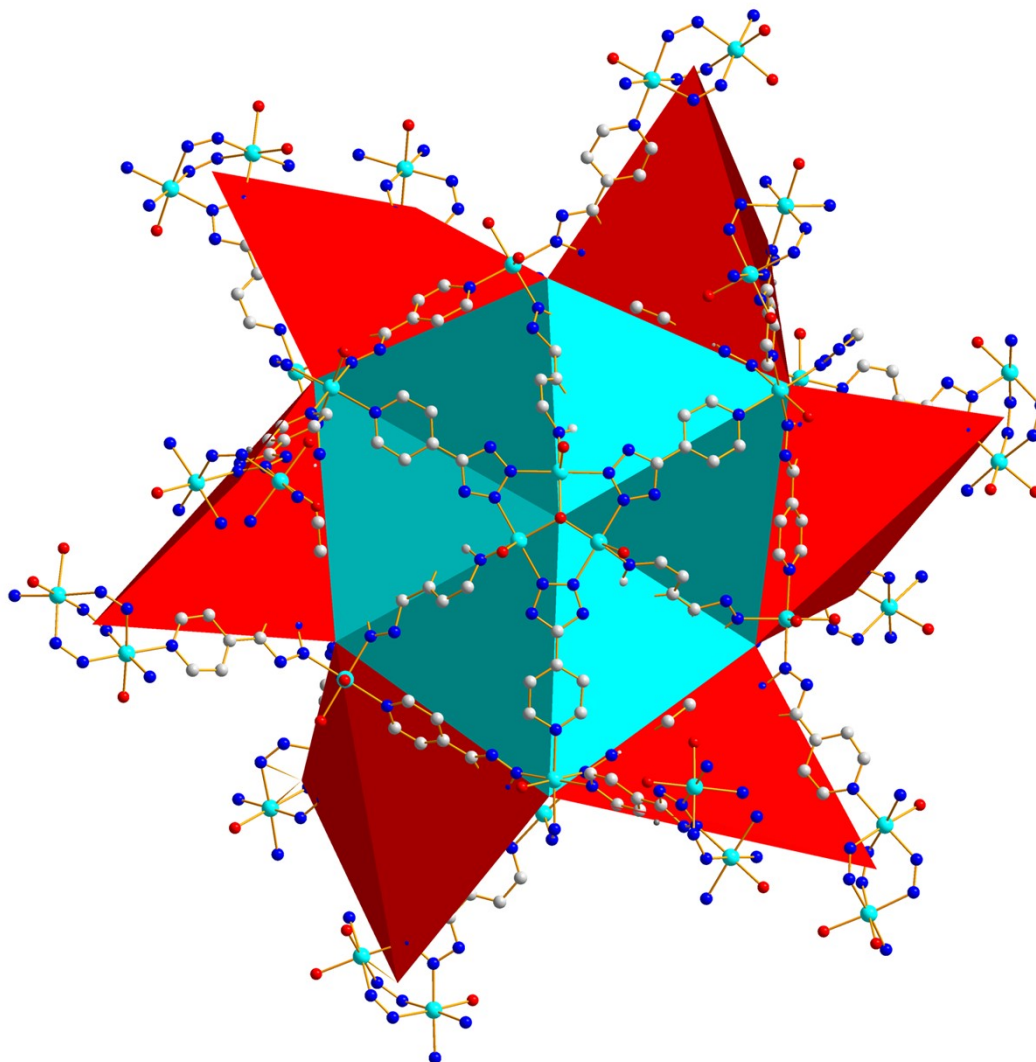


Fig. S5 Six-vented windmill built by double-vertex shared mode of twisted quadrangle in GMOF-1.

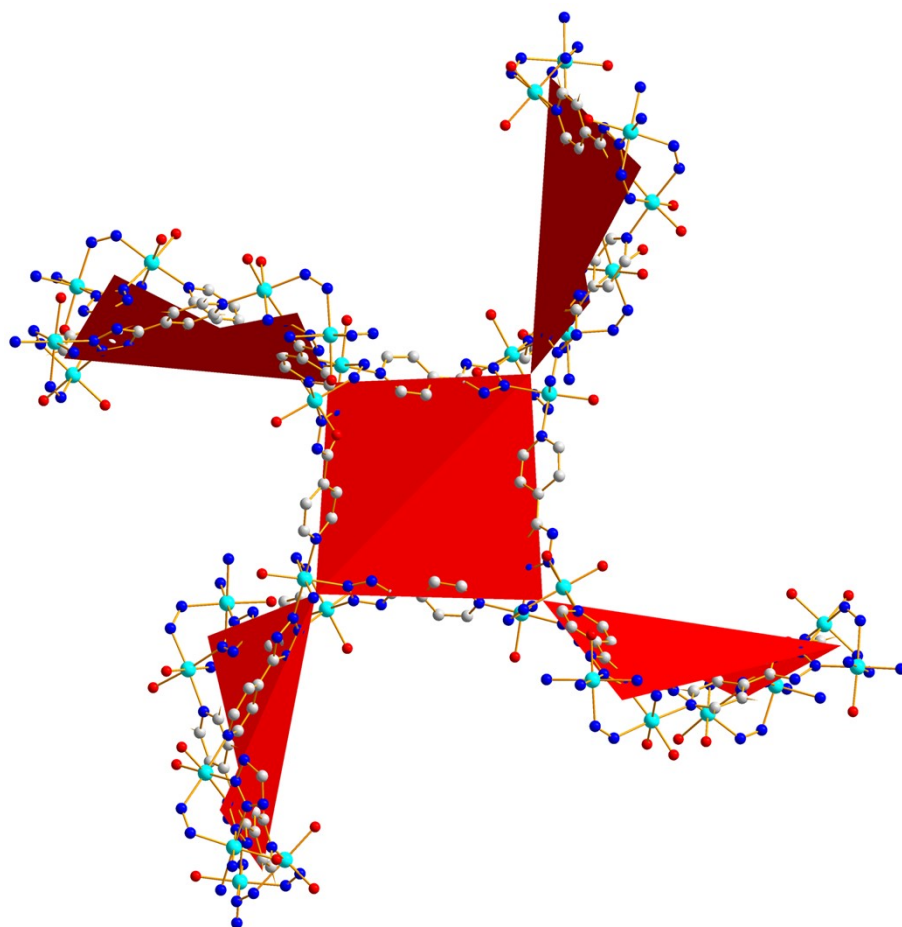


Fig. S6 Single-vertex linkage mode of twisted quadrangle in GMOF-1.

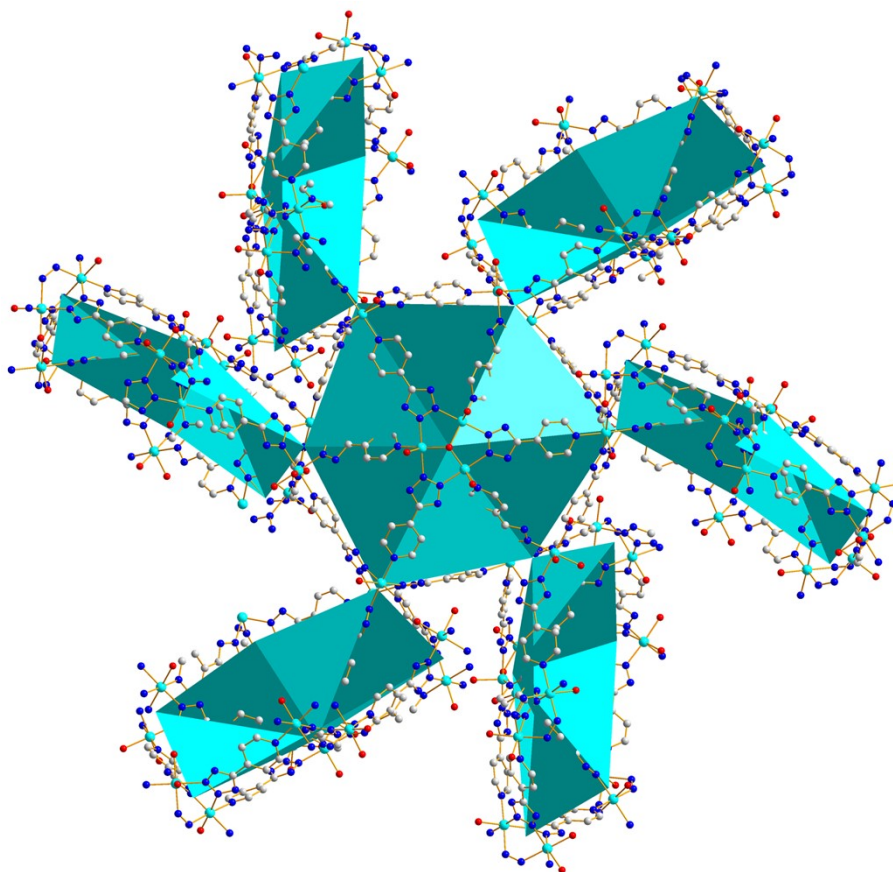


Fig. S7 Single-vertex linkage mode of non-planar hexagon in GMOF-1.

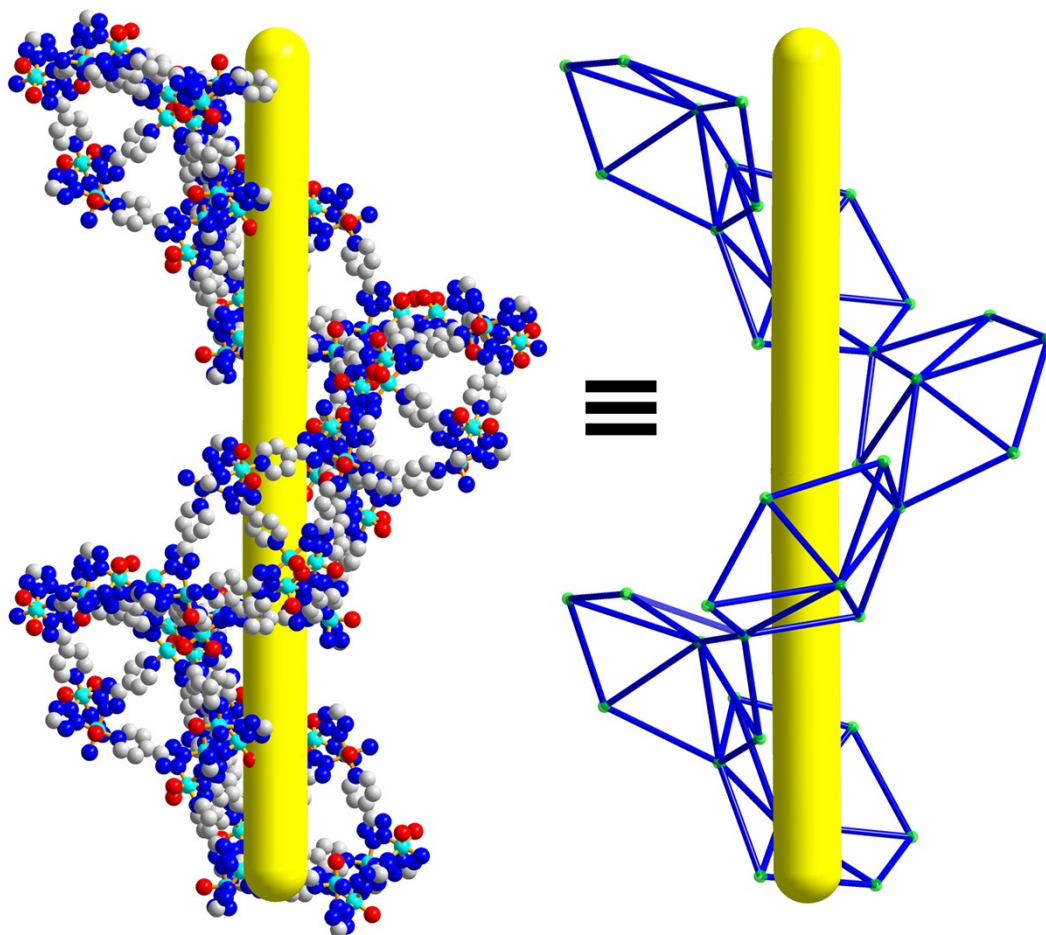


Fig. S8 Right-handed channel exhibition through vertex-sharing connection of non-planar hexagons in GMOF-1.

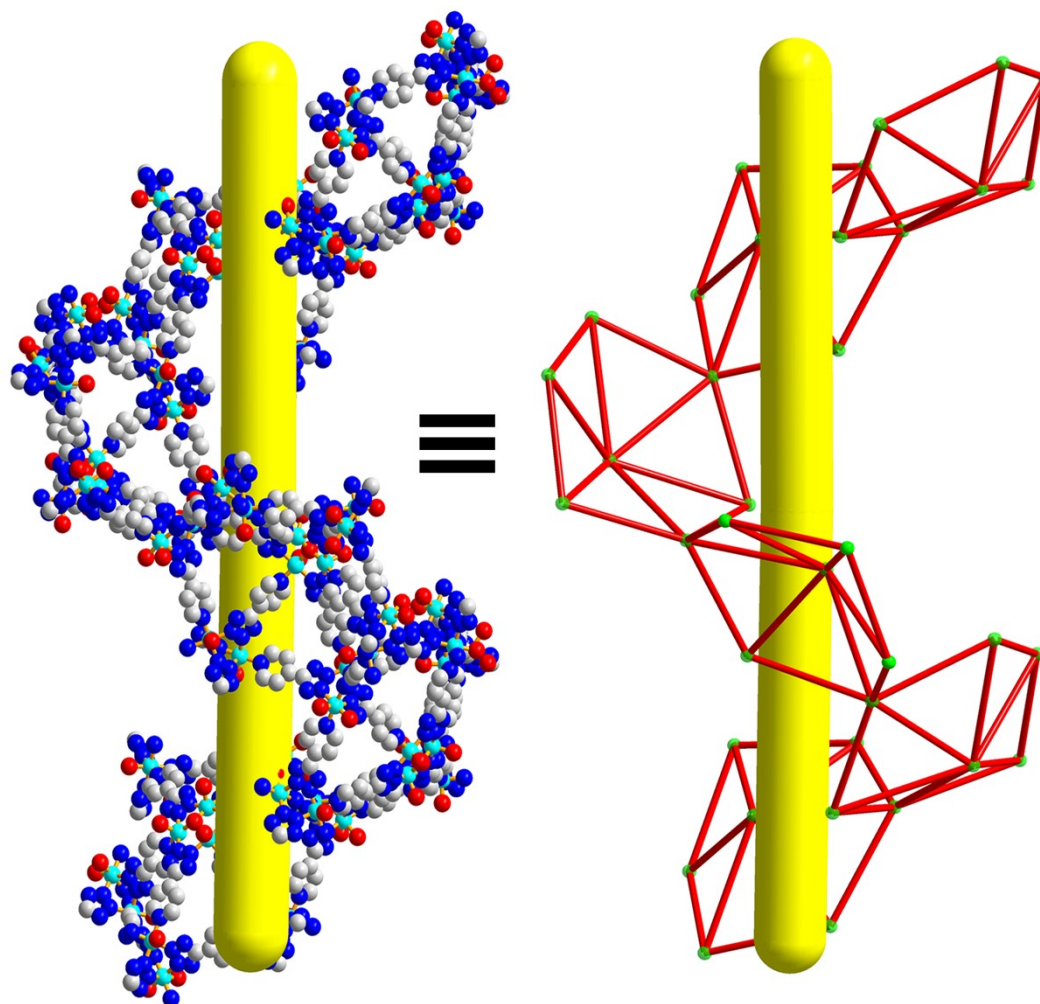


Fig. S9 Left-handed channel exhibition through vertex-sharing connection of non-planar hexagons in GMOF-1.

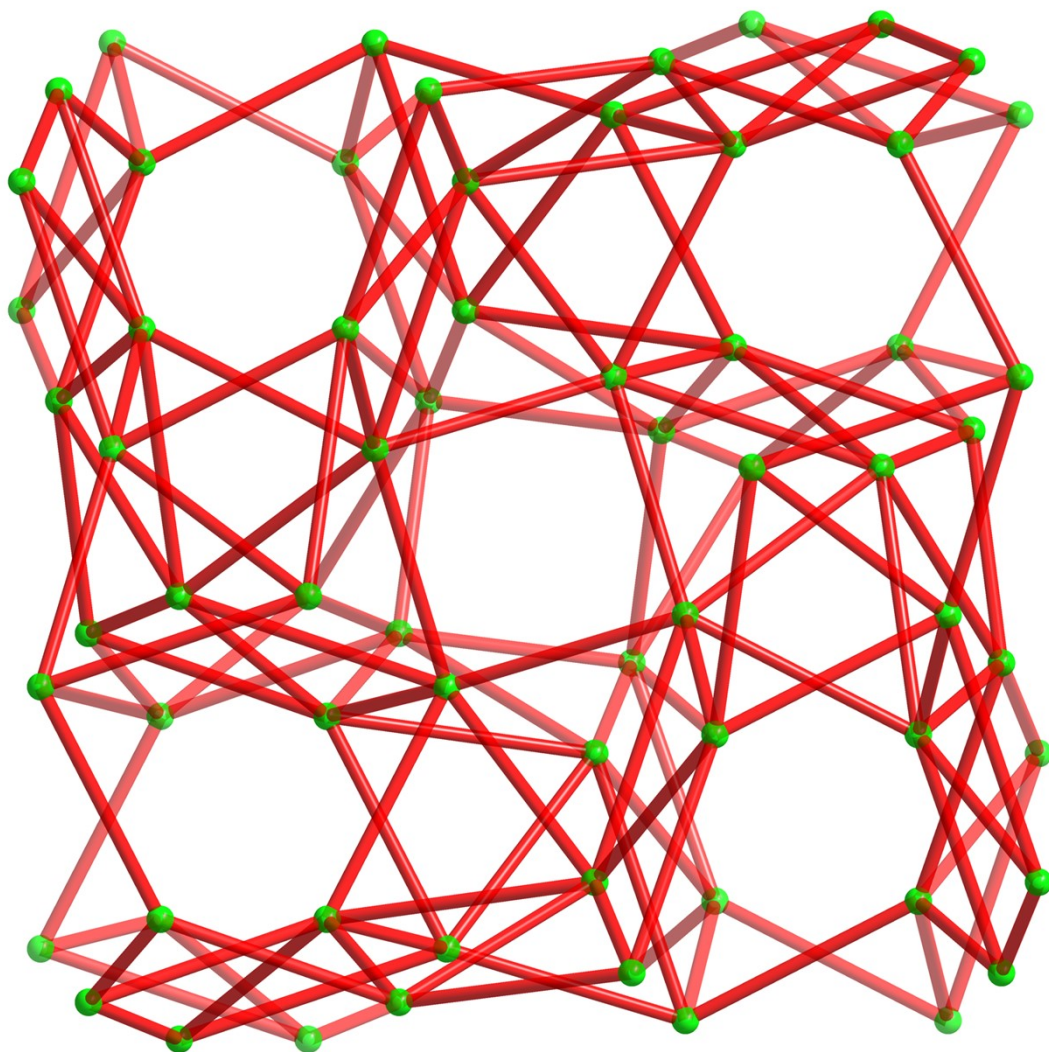


Fig. S10 The topological presentation of GMOF-1 in *a* axis.

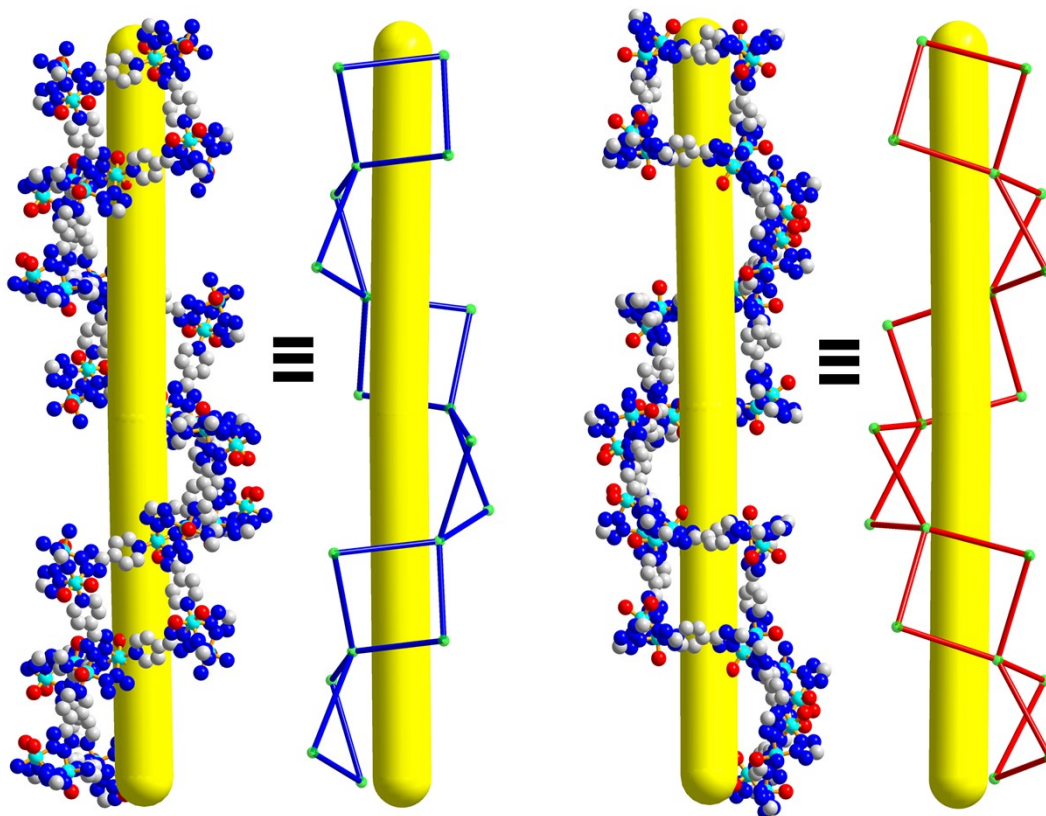


Fig. S11 Helical channels exhibition through vertex-sharing connection of twisted quadrangles of GMOF-1.

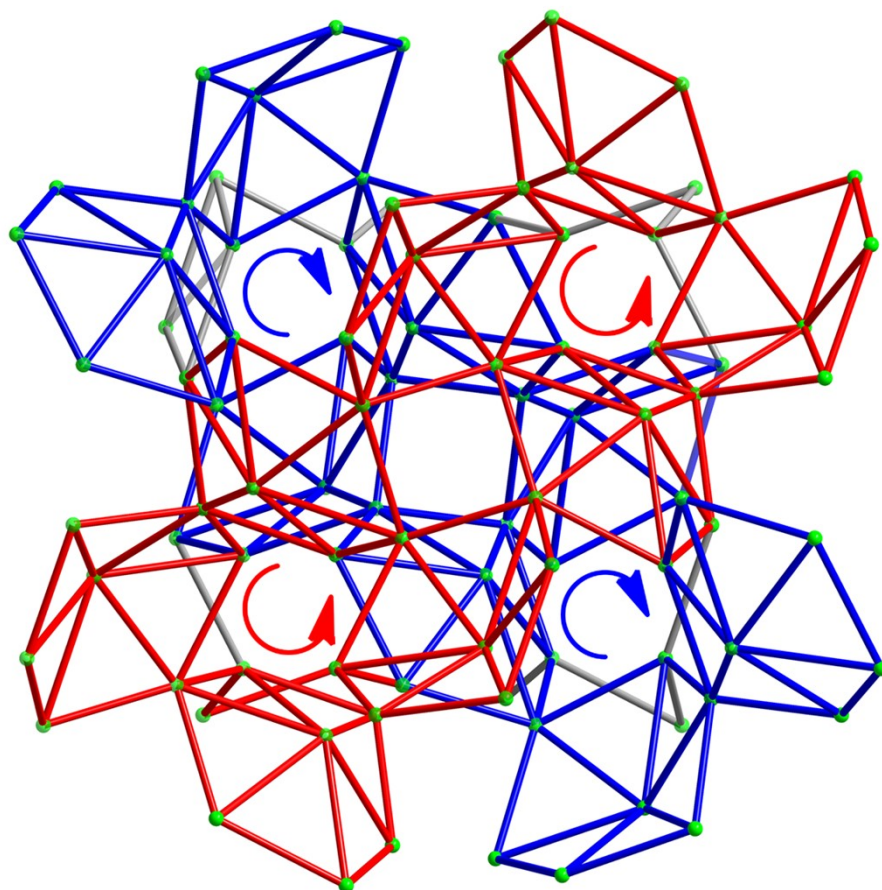


Fig. S12 The exhibition of the helical channel in GMOF-1 through vertex connection of non-planar hexagons.

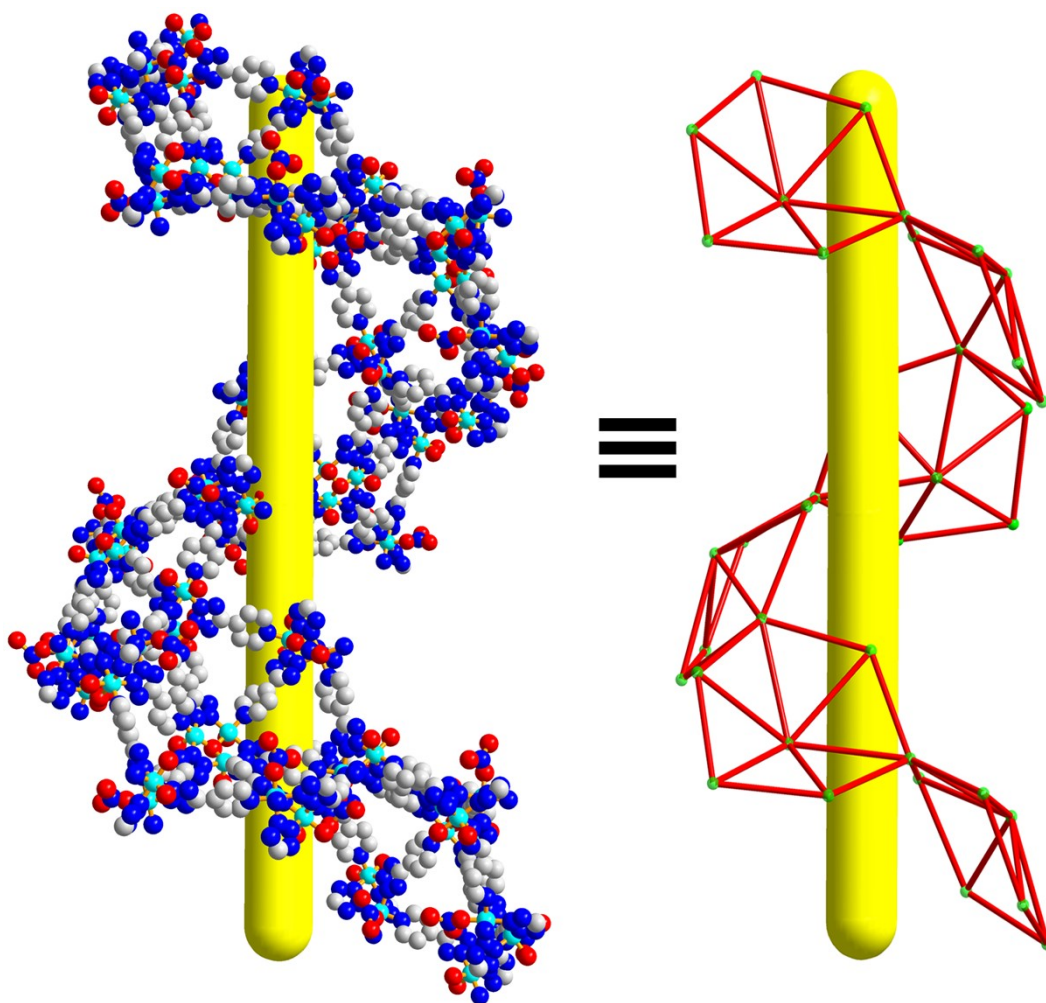


Fig. S13 Left-handed channel exhibition through vertex-sharing connection of non-planar hexagons in GMOF-3.

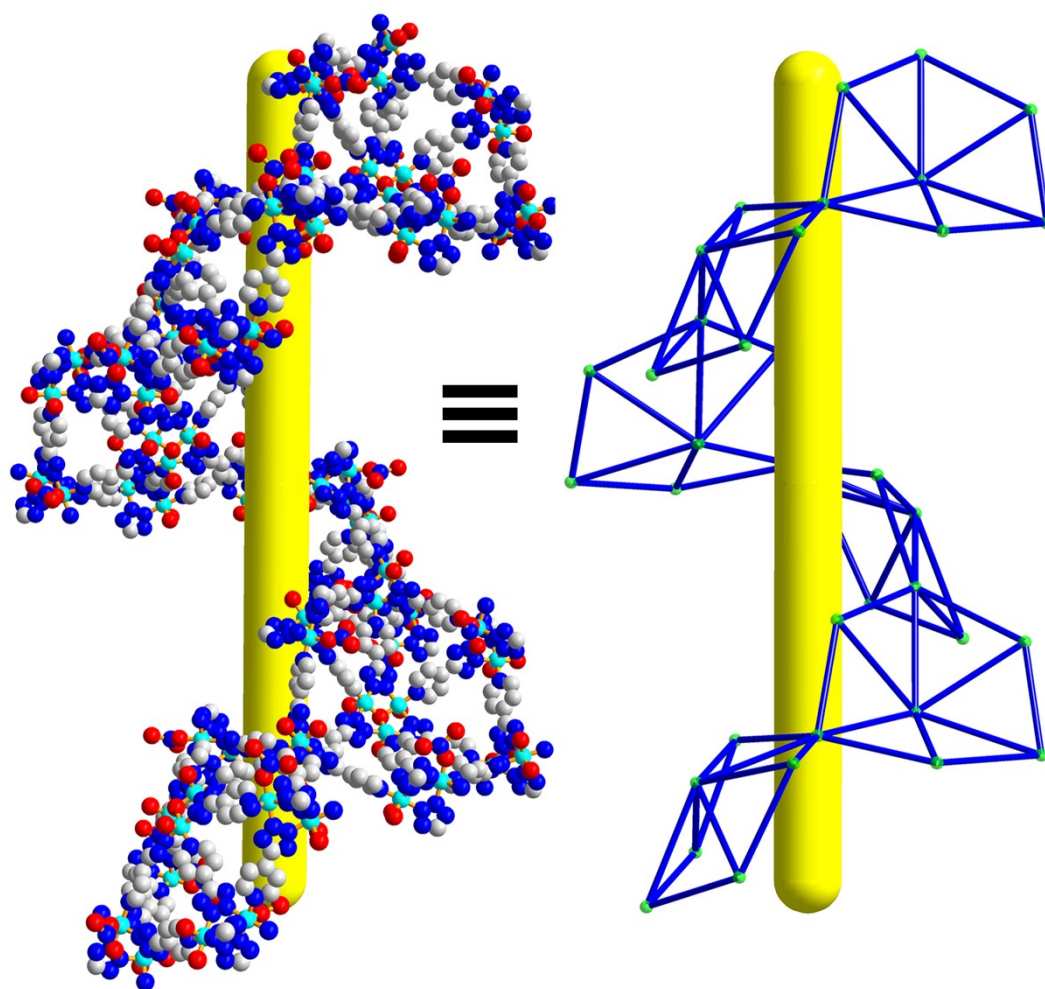


Fig. S14 Right-handed channel exhibition through vertex-sharing connection of non-planar hexagons in GMOF-3.

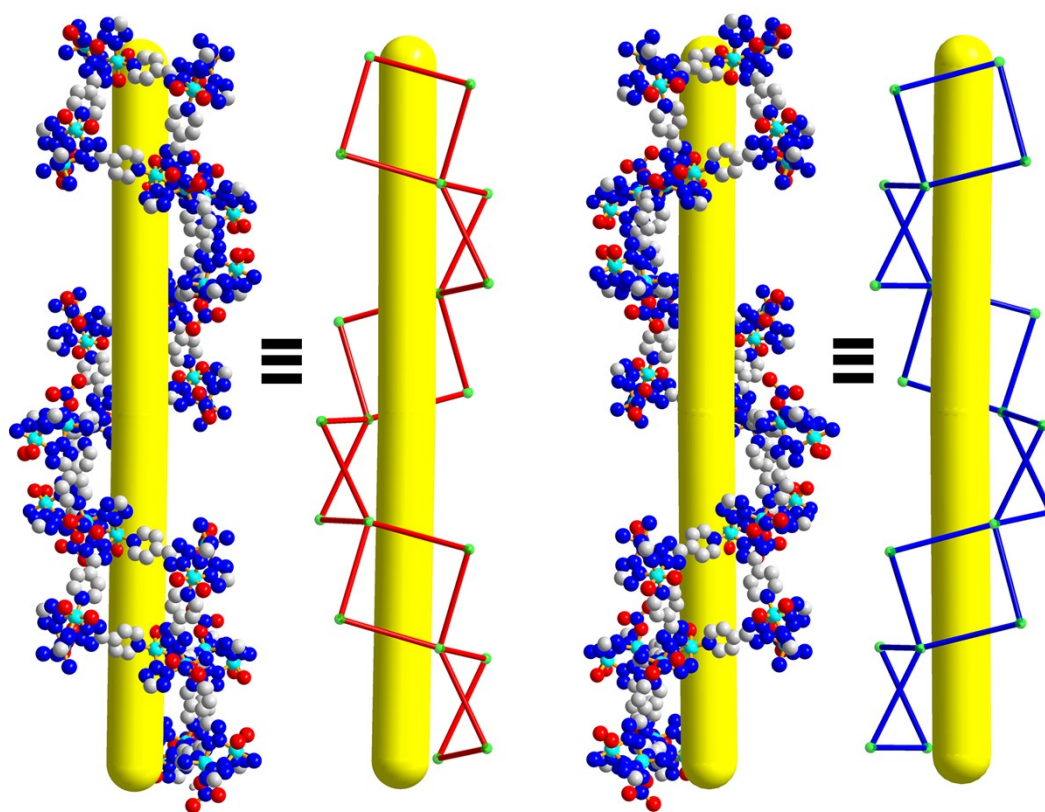


Fig. S15 Helical channels exhibition through vertex-sharing connection of twisted quadrangles of GMOF-3.

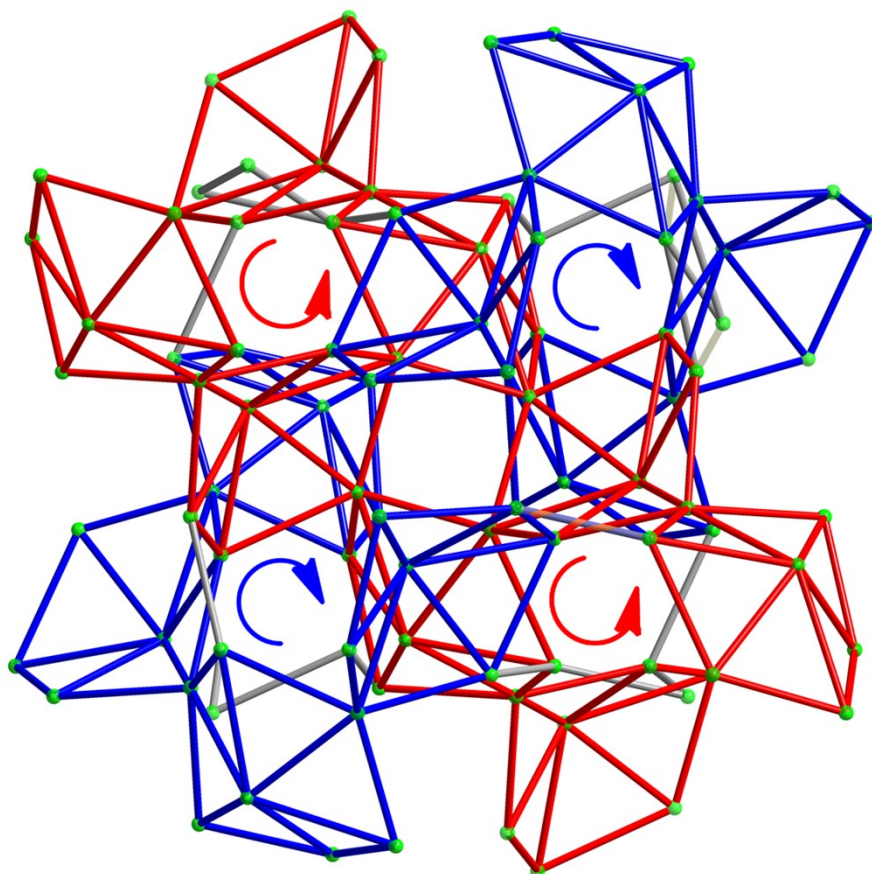


Fig. S16 The presentation of helical channel in GMOF-3 through vertex connection of non-planar hexagons.

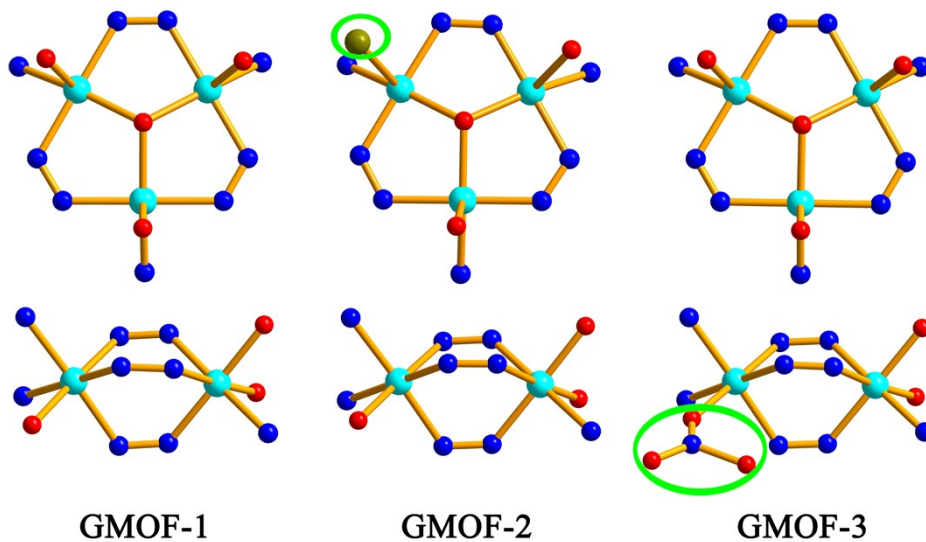


Fig. S17 Left: coordinated environments of SBUs in GMOF-1; Middle: coordinated environments of SBUs in GMOF-2; Right: coordinated environments of SBUs in GMOF-3 (gray C, blue N, red O, turquoise Co, dark yellow Br).

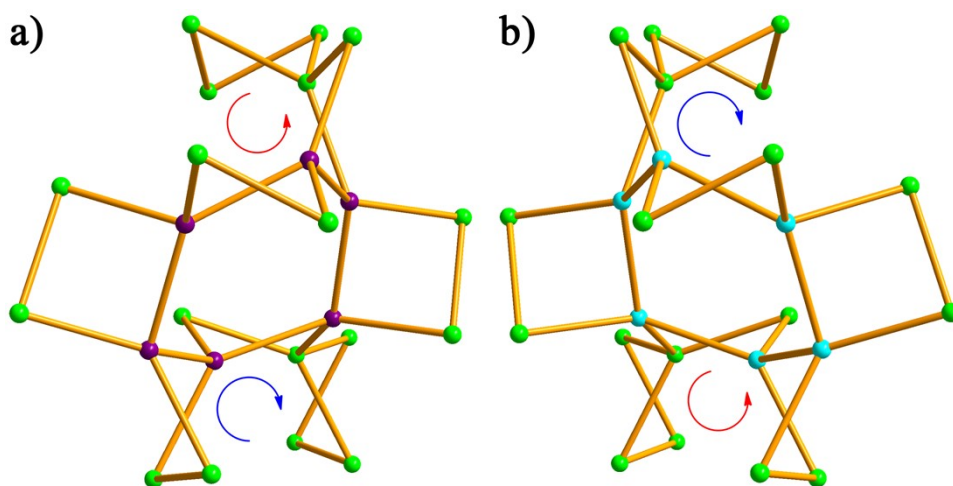


Fig. S18 Inverse channel presentation in GMOF-1 (a) and (b) GMOF-3 containing asymmetric unit in a axis (green: SBU(II) in twisted quadrangle; violet: SBU(II) in hexagonal concave of GMOF-1; light blue: SBU(II) in hexagonal concave of GMOF-3).

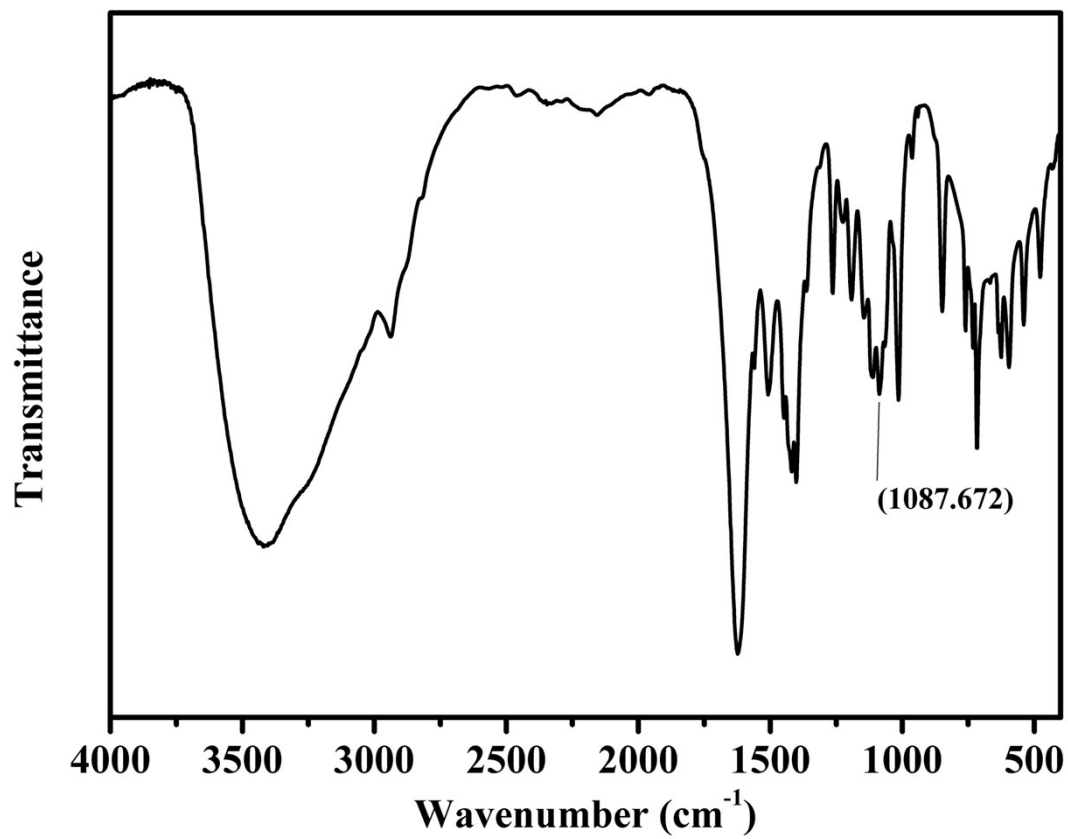


Fig. S19 IR spectrum of GMOF-1.

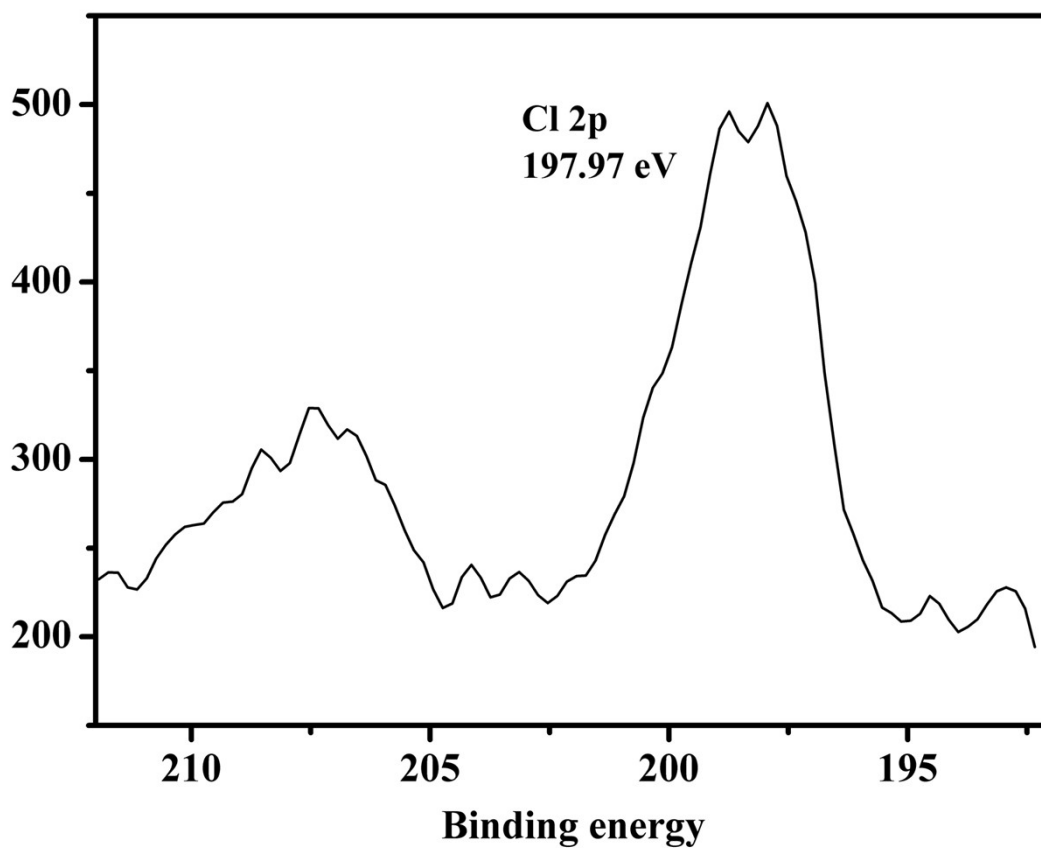


Fig. S20 XPS spectrum of GMOF-1.

Table S3 Relative atomic ratio of GMOF-1 through XPS spectrum.

Element	C1s	N1s	O1s	Cl2p	Co2p3
Atomic Ratio	57.82	26.27	8.97	2.1	4.84
Binding Energy (eV)	284.80	399.27	531.61	197.97	780.94

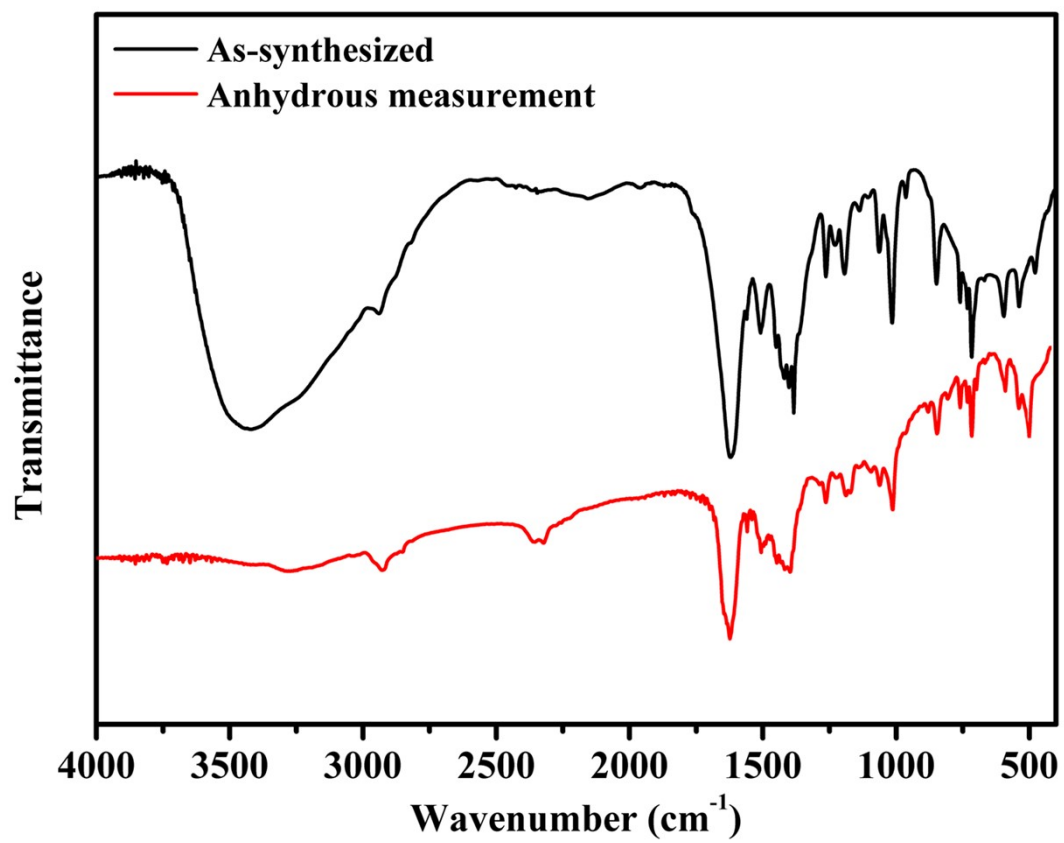


Fig. S21 IR spectra of GMOF-2.

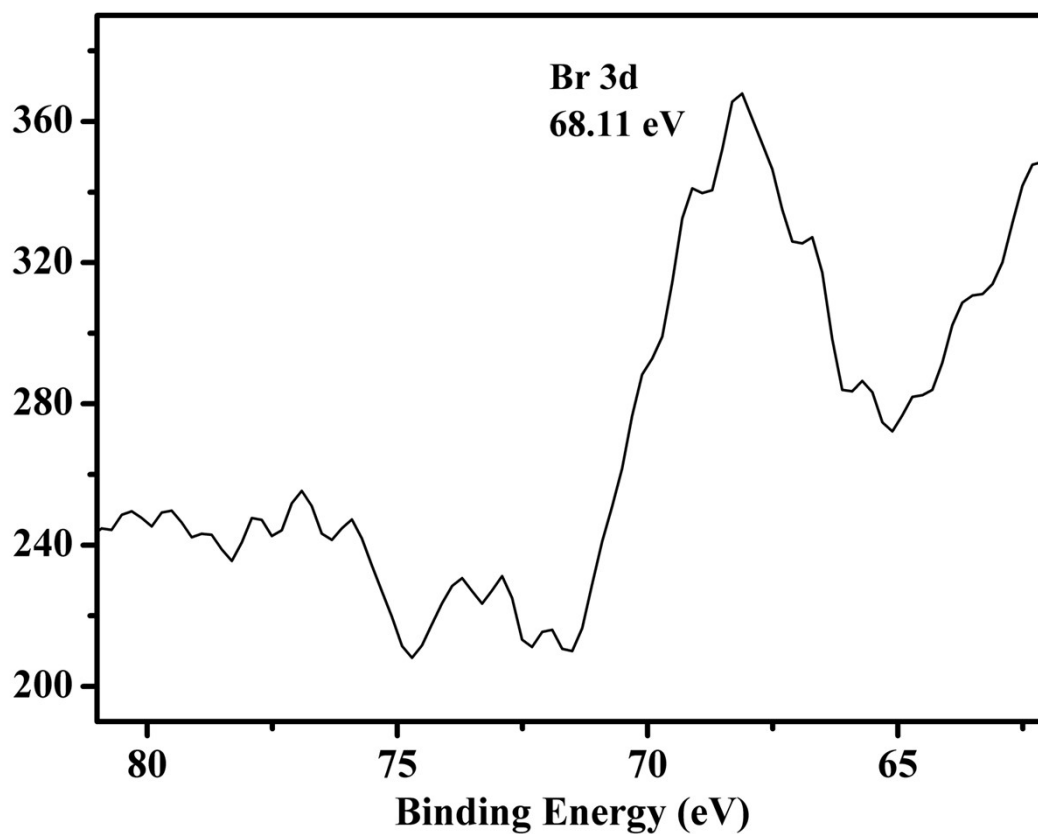


Fig. S22 XPS spectrum of GMOF-2.

Table S4. Relative atomic ratio of GMOF-2 through XPS spectrum.

Element	C1s	N1s	O1s	Co2p3	Br3d
Atomic Ratio	66.12	21.27	8.35	3.75	0.44
Binding Energy (eV)	284.80	399.66	532.28	781.06	68.11

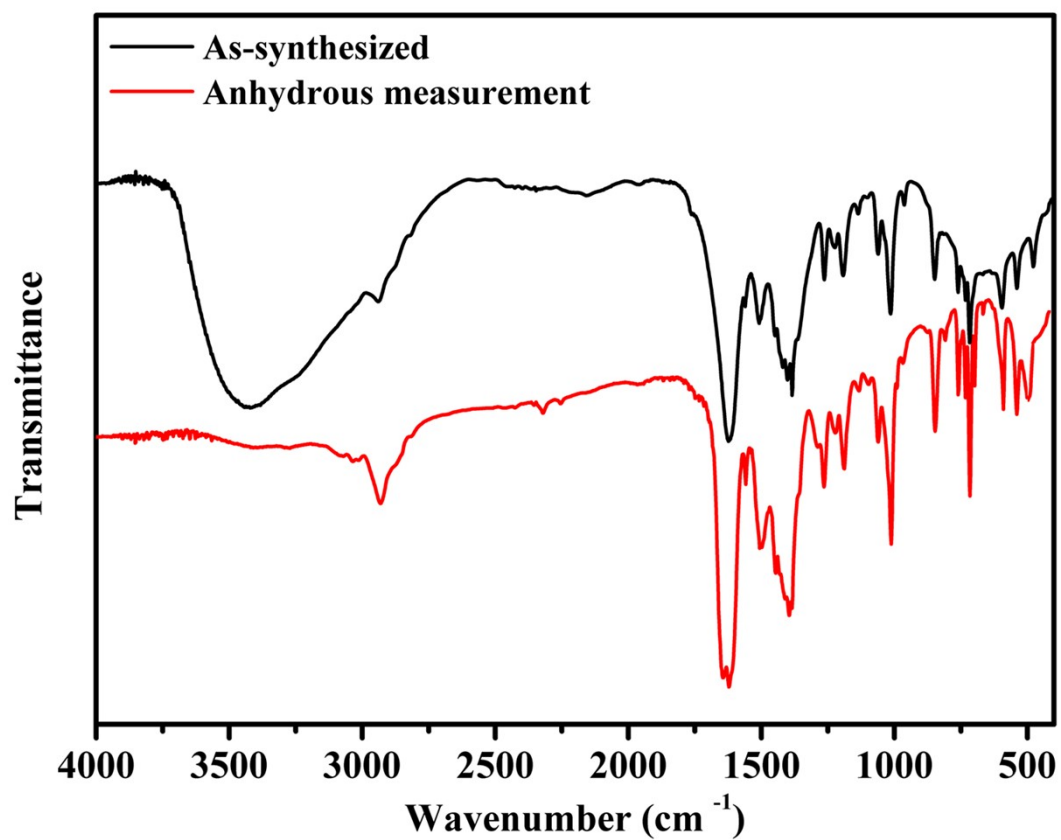


Fig. S23 IR spectra of GMOF-3.

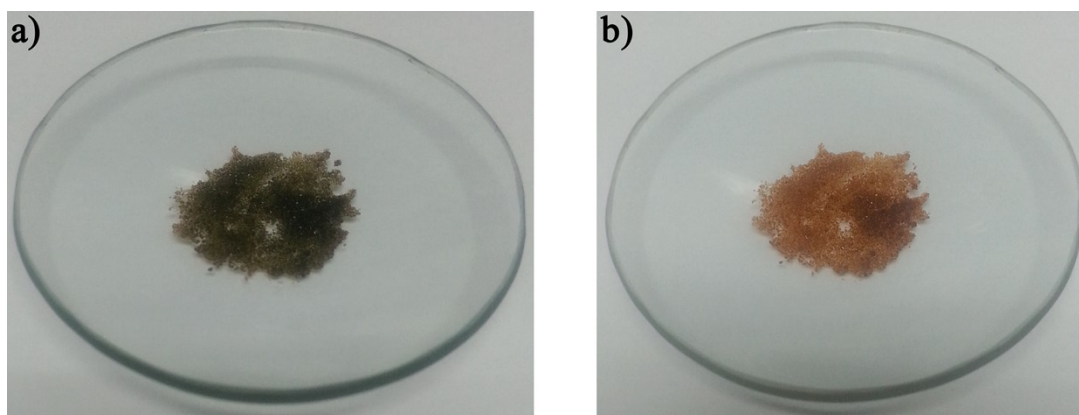


Fig. S24 (a) Fresh sample of GMOF-2, (b) Color change of GMOF-2 as exposed to moist air for few minutes.

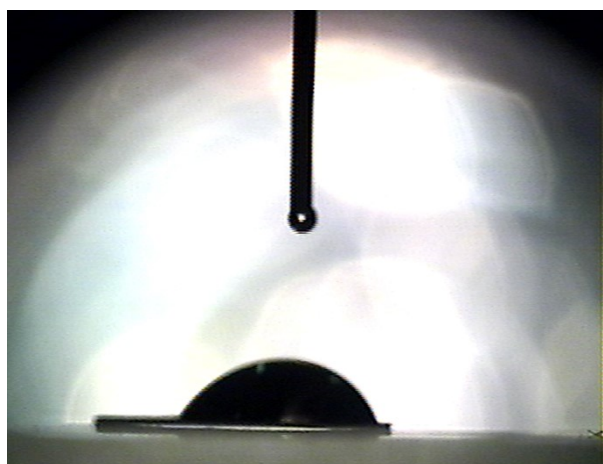


Fig. S25 Static contact angle of water of GMOF-2.

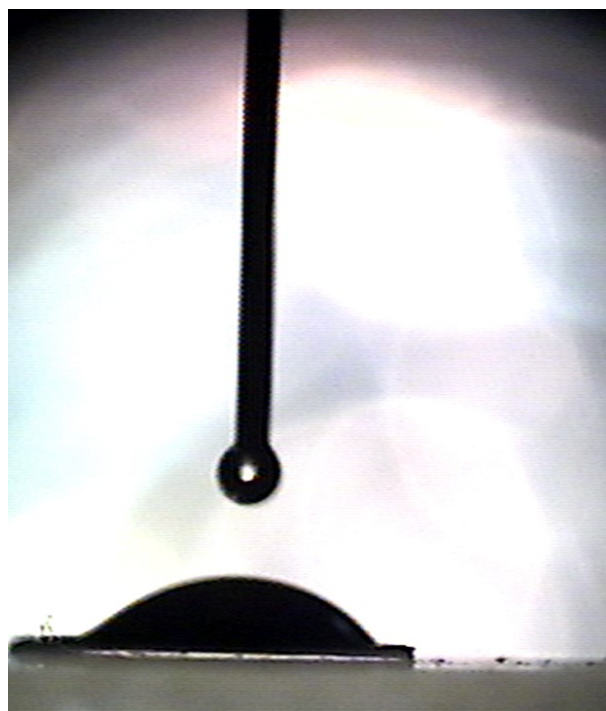


Fig. S26 Static contact angle of water of GMOF-3.

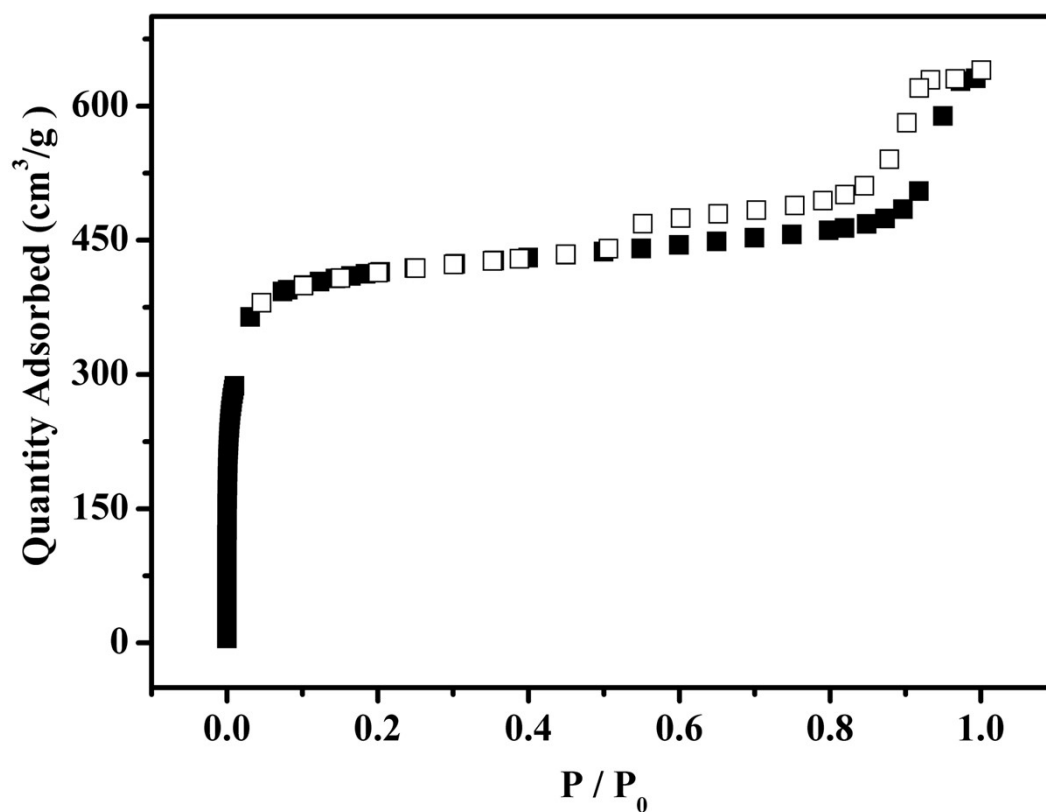


Fig. S27 N_2 adsorption isotherm of GMOF-2 at 77 K.

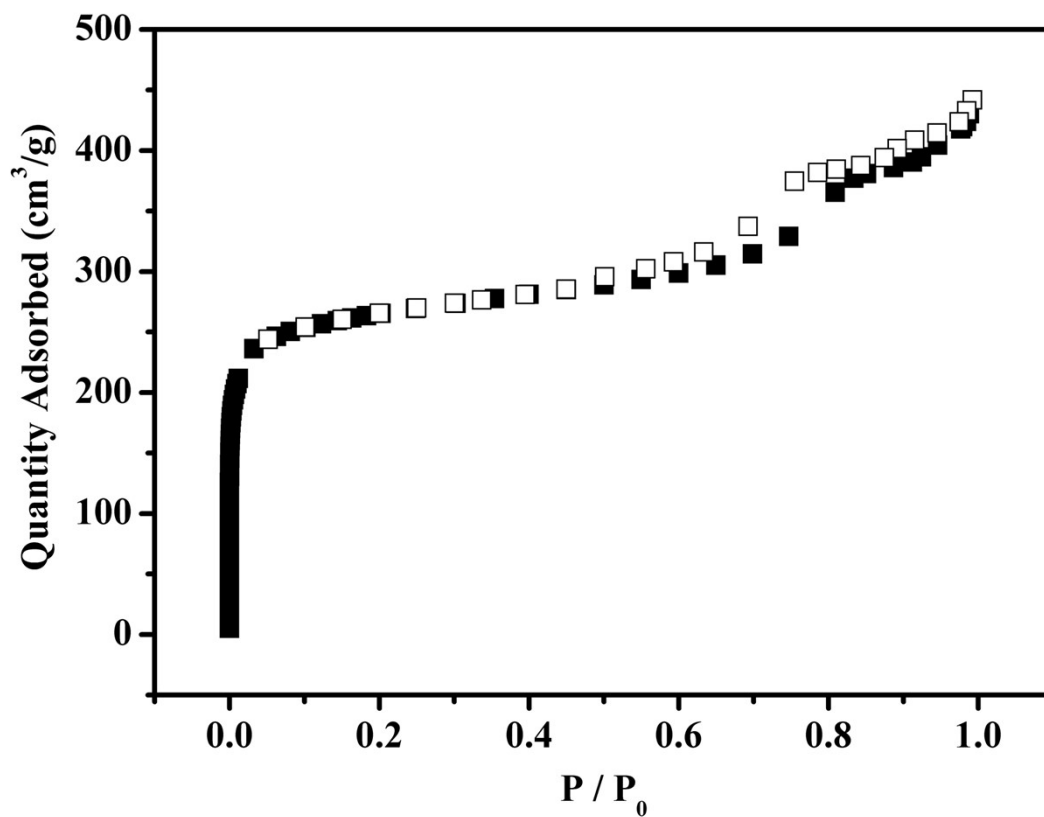


Fig. S28 N₂ adsorption isotherm of GMOF-3 at 77 K.

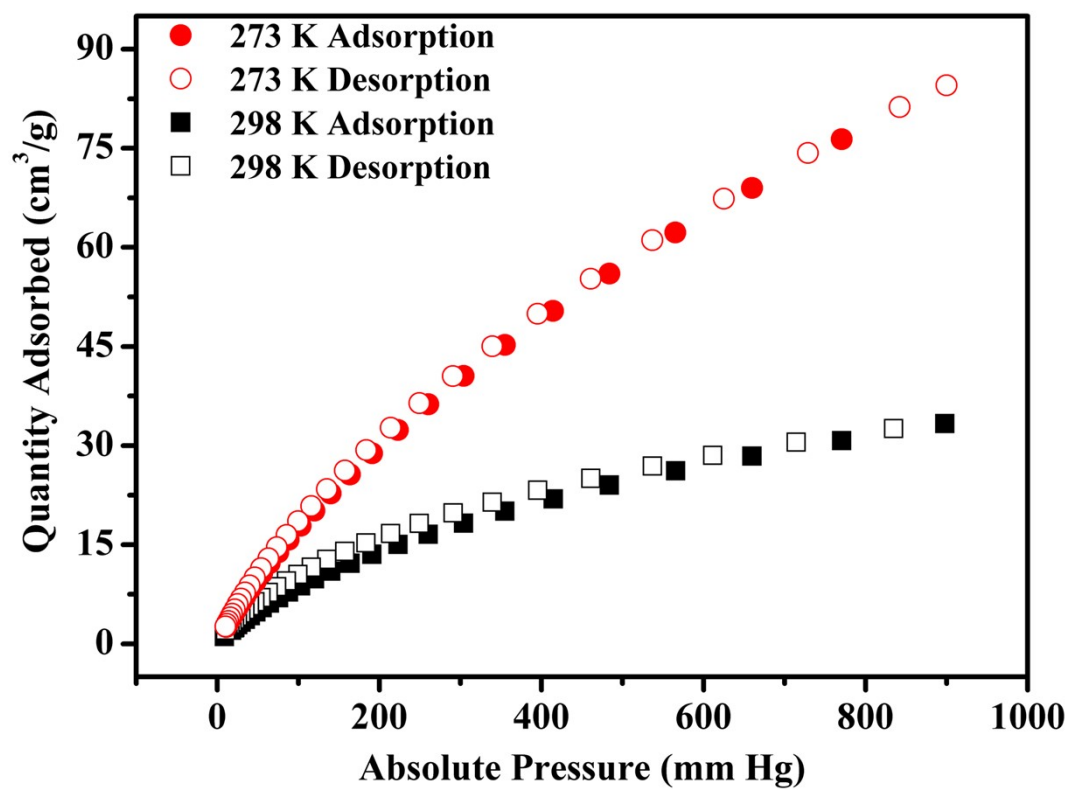


Fig. S29 CO₂ adsorption isotherms of GMOF-2.

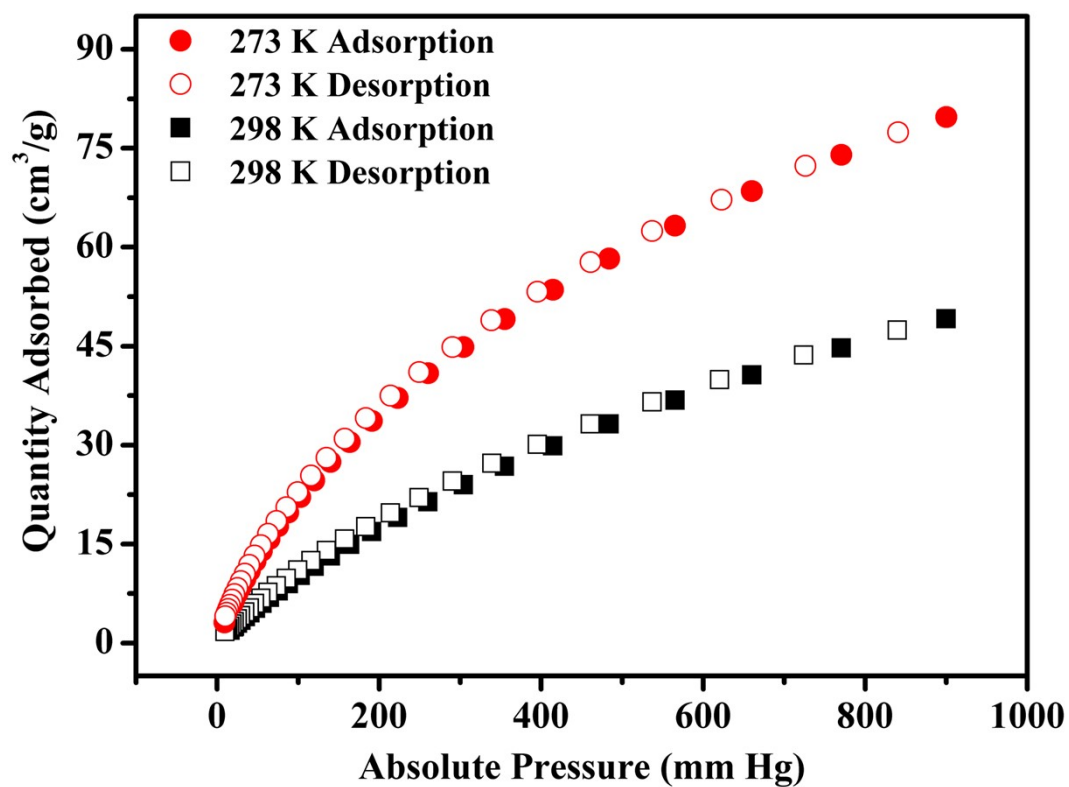


Fig. S30 CO₂ adsorption isotherms of GMOF-3.

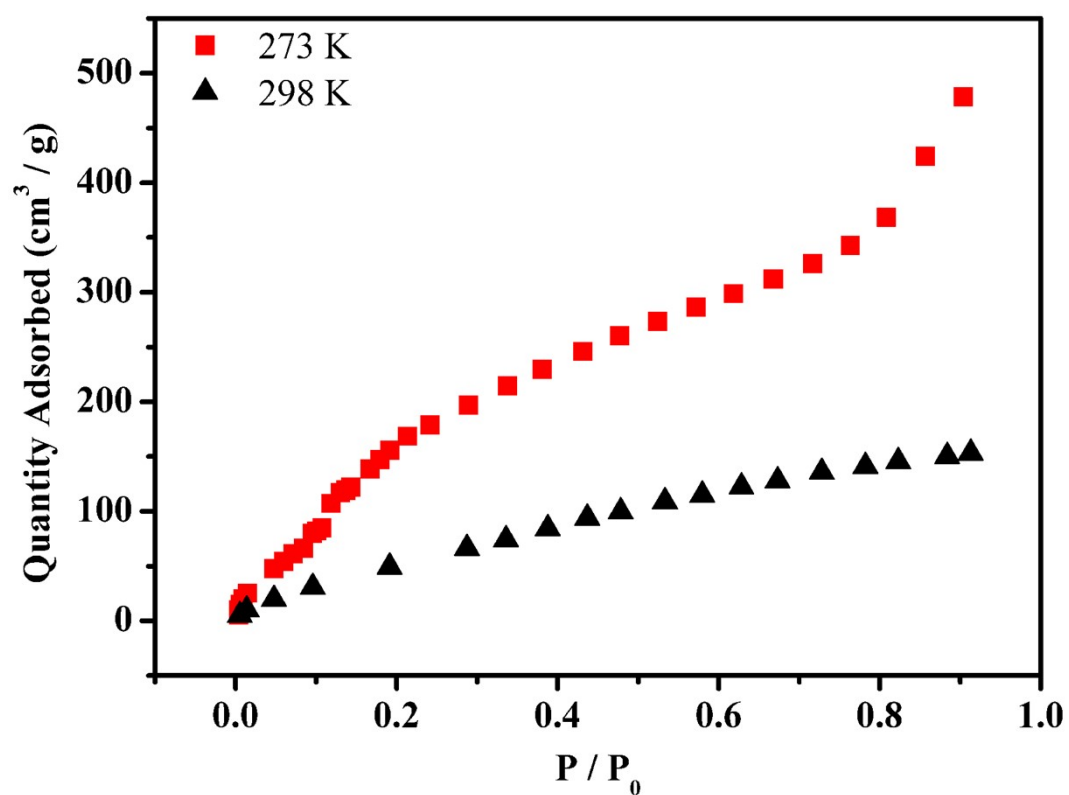


Fig. S31 H₂O adsorption isotherms of GMOF-2.

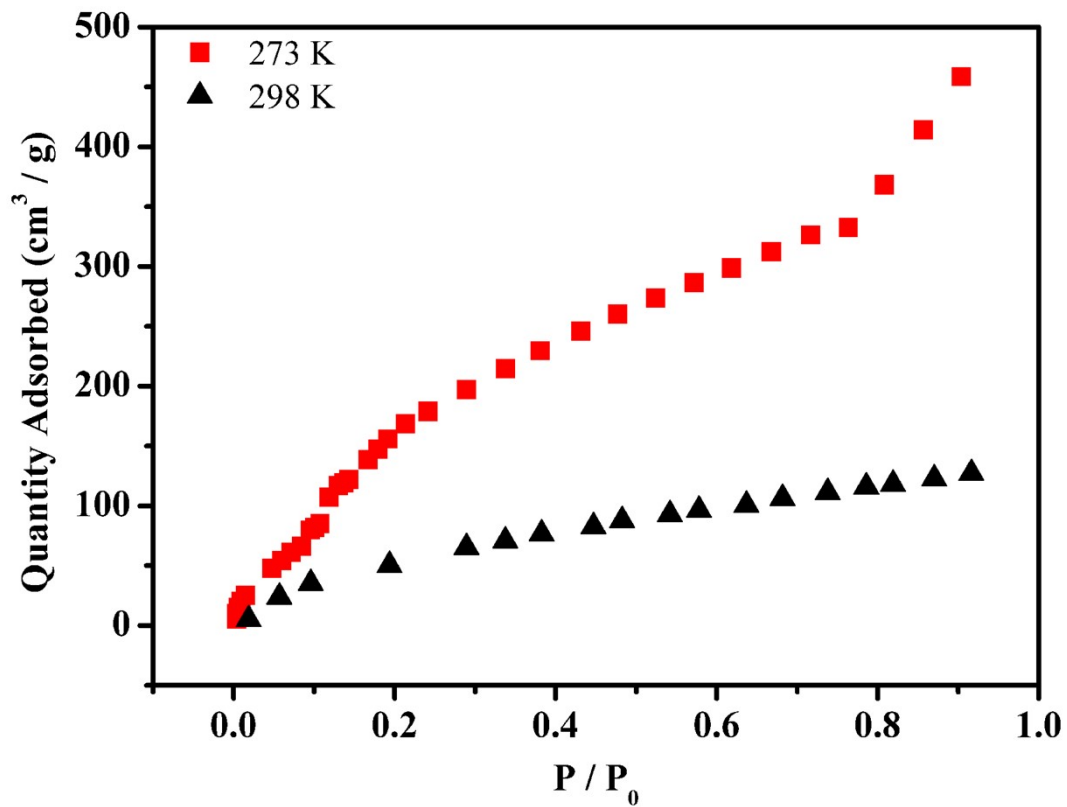


Fig. S32 H₂O adsorption isotherms of GMOF-3.